Pergamon

Journal of Structural Geology, Vol. 17, No. 5, pp. 739 to 750, 1995
Elsevier Science Ltd
Printed in Great Britain
0191-8141/95 $9.50+0.00

0191-8141(94)00089-1

The Mohr circle for curvature and its application to fold description

RICHARD J. LISLE and JULIAN M. ROBINSON

Laboratory for Strain Analysis, Department of Earth Sciences, The University of Wales, Cardiff CF2 3YE, U.K.

(*Received* 23 *November* 1993; *accepted in revised form* 4 *August* 1994)

Abstract—Most conventional methods for the analysis of fold structures are founded on the assumption of cylindricity. It has been repeatedly shown that these methods can be useful for dealing with a wide range of structural geometries, even those for which the assumption is only approximately valid, e.g. structures produced by the interference of superimposed fold sets. In some instances though, such as in the analysis of oil-field structures, it is the presence and type of non-cylindricity in a structure which is of primary interest. The description of such folded surfaces requires more general methods of analyzing surface curvature based on the principles of differential geometry. The Mohr circle construction, already familiar to structural geologists in the context of stress and strain, is shown to be useful for the analysis of surface curvature and torsion. A practical method of mapping principal curvatures and their trajectories, involving the application of the Mohr circle, is described and applied, by way of example, for the survey of the Goose Egg Dome in Wyoming and a small-scale fold from Laksefjord, Norway.

INTRODUCTION

The description of folded surfaces for geological purposes is usually accomplished with reference to the cylindrical fold model. A cylindrical fold is one which yields identical cross-sections when sectioned serially. For this reason the model can be thought of as essentially two-dimensional; the important features of the surface's geometry (e.g. fold tightness) are portrayed in any single section plane parallel to the line of greatest curvature. Terms such as *hinge line, true profile* and *inflection line* have definitions which assume, often implicitly, that the folds concerned are cylindrical. In spite of the restrictions of the model, natural folds approximate cylindrical geometry sufficiently closely, and sufficiently often, to make this simple approach to fold description practicable.

With some structures however the cylindrical model is less adequate. These include some of the structures produced by non-coaxial refolding (domes, basins, periclines) and some weakly developed structures of low amplitude. Even in such cases the cylindrical fold approach is sometimes still used, by taking small enough patches or domains and analyzing them separately (Turner & Weiss 1963, pp. 148, 171). The justification for this lies in the assumption that a structure which is non-cylindrical consists of smaller portions which are more cylindrical. It is not difficult to visualize structures for which this assumption is invalid.

This paper suggests a general technique for analyzing folded surfaces that is free of assumptions regarding the degree of cylindricity possessed by the structure. The method, which by necessity is three-dimensional since there need be no direction along which the structural geometry remains constant, analyses the folded surface by determining the local state of curvature at points distributed across the surface. For the calculation of curvature at points on a surface the Mohr circle construction is found to be useful. The representation of curvature determined by this method leads to a form of display which is complementary to the structure contour map, the traditional way of representing the geometry of non-cylindrical folds.

The structure contour map is probably the most commonly used type of display for representing non-cylindrically folded surfaces. Such maps allow the ready identification of certain fold features. In particular, those features relating to relative elevation of points such as the position of *culmination points, depression points, crest lines* and *trough lines* and the relative steepness of dips at different points on the surface can be directly appreciated. The positions of these features on any folded surface however are influenced by the overall orientation of the surface with respect to the horizontal and for this reason are not features which are useful for defining the intrinsic geometry of a surface (Ramsay 1967, p. 346). The main limitation of the structure contour map is its inability to represent the more important, rotation-invariant property of curvature.

In the case of cylindrical folds the definitions of most of the important features of a fold depend on curvature (e.g. *hinge* and *inflection lines* and dependent features such as *limb, interlimb angle, wavelength*, etc.). Although the corresponding terms for non-cylindrical folds are not yet defined, the property of curvature is likely to be important in relation to the mechanics of the folding process and the occurrence of strain-related features associated with folds. For example it has been suggested that the curvature of non-cylindrical folds may relate to the strains within the plane of the bedding produced during folding (Lisle 1992a).

CURVATURE OF SURFACES

The geometrical theory of surfaces has seldom been applied to geological folds, though the potential for such applications is pointed out in the texts by Ramsay (1967, pp. 345–347) and Suppe (1985, pp. 311–313). A wealth of relevant literature exists in the field of differential geometry (e.g. Kreysig 1964, O'Neill 1966, Lipschutz 1969, Calladine 1986, Nutbourne & Martin 1988) of which Hilbert & Cohn-Vossen (1932) and Koenderink (1990) are particularly accessible for the non-mathematician.

In a cylindrical fold the curvature at any point on the surface is unambiguously defined by means of single value (scalar) calculated as the reciprocal of the radius of curvature of the section of the surface seen in true profile (Fig. 1a).

In non-cylindrically folded surfaces the situation is more complicated because the profile plane is not defined for this type of surface. The curvature measured depends on the direction of the curve considered (Fig. 1b). There is an analogy here with stress and its components acting on planes passing through a given point P, where the normal and shear stress components vary depending on the orientation of the plane considered. Like stress, curvature at a point on any surface can be described by means of a second-order tensor. Before discussing the nature of the tensor it is necessary to explain different ways of defining curvature.

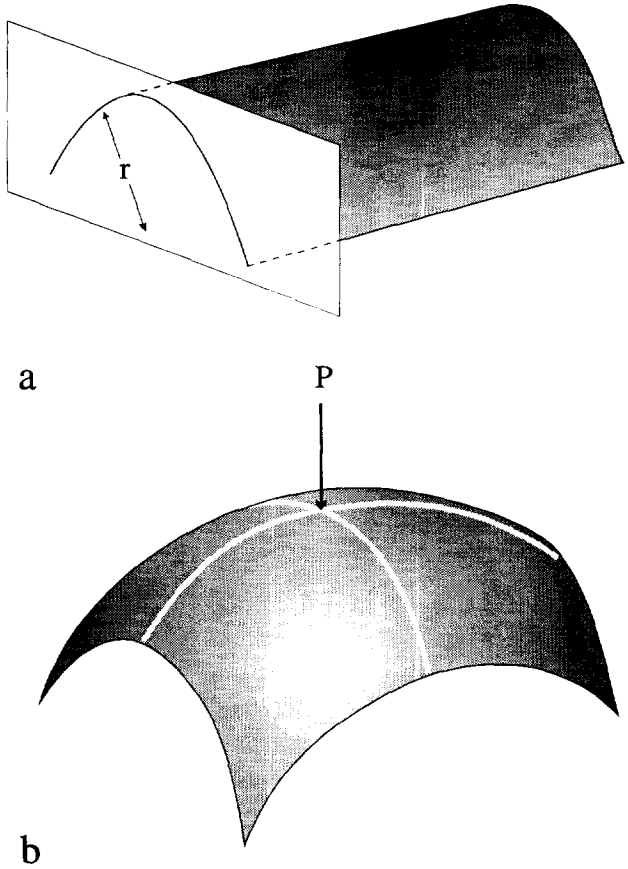

Fig. 1. Curvature of surfaces (a) cylindrical fold. Curvature (k) at a given point is represented by a scalar equal to the reciprocal of the radius of curvature measured on the fold's true profile (b) general surface. No true profile exists, curvature at a point P depends on the section plane being considered.

Space curves

Some important geometrical properties of surfaces are described by means of the properties of curves which lie within them. For this reason the discussion of surfaces has to be preceded by the mention of curves as separate entities, without reference to the surface on which they lie. Curves described in these terms are called *space curves* (Nutbourne & Martin 1988, pp. 16–72).

Figure 2 shows an example of a space curve. At any point P along it, three unit vectors can be defined. These three vectors define a reference frame for describing the curve at P. This is called the *space curve frame*.

The first of the three vectors which define the space curve frame is the line of tangency **t** of the curve at P. The second is defined with reference to the plane which, locally at P, contains the curve. This plane, called the *osculating plane*, can be defined as the limiting position of a plane passing through P and two points on the curve at opposite sides of P as these points approach P. This plane contains **t** and the second unit vector, **n** which is perpendicular to **t**. The third vector, **b**, the so-called *binormal vector* (Fig. 2), is the direction normal to the osculating plane.

The three orthogonal axes that define the space curve frame, change orientation as we move away from P along the curve. The *moving trihedron* is the name given to the assembly of three planes (the planes normal to **t, n** and **b**, respectively) which bodily rotates with changing position along the space curve.

At P the *curvature of a space curve*, k, is the rate of change of the direction of the tangent vector **t** with distance s along the curve (Fig. 3a). It measures the deviation of the curve from a straight line in the neighbourhood of P. By definition, the curvature of the space curve is displayed in the osculating plane. In the immediate vicinity of P the curve is an arc of a circle in the osculating plane with radius r. The latter is called *radius of curvature* and can be used to calculate the curvature k of the space curve:

$$k = 1/r. \qquad (1)$$

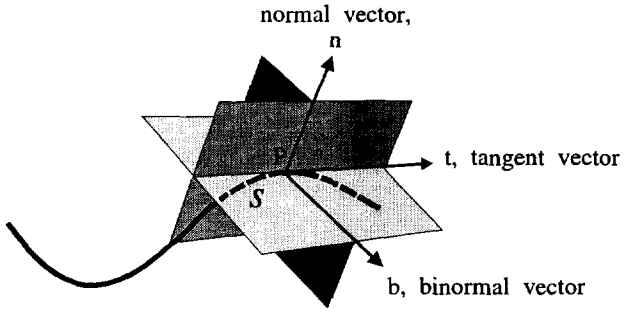

Fig. 2. A space curve and the space curve trihedron at a point P at a certain distance s along it. Trihedron is defined by the orthogonal vectors **t, n** and **b**. Plane containing the normal **n** and tangent **t** is also the plane containing the space curve locally at P.

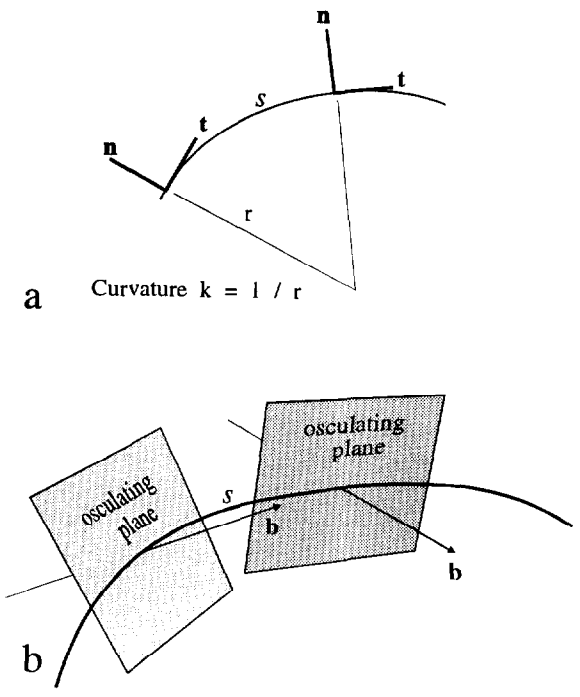

Fig. 3. Properties of a space curve. (a) Curvature is the rate of change of **t** with distance along the curve. (b) Torsion is the rate of change of **b** with distance s along the space curve.

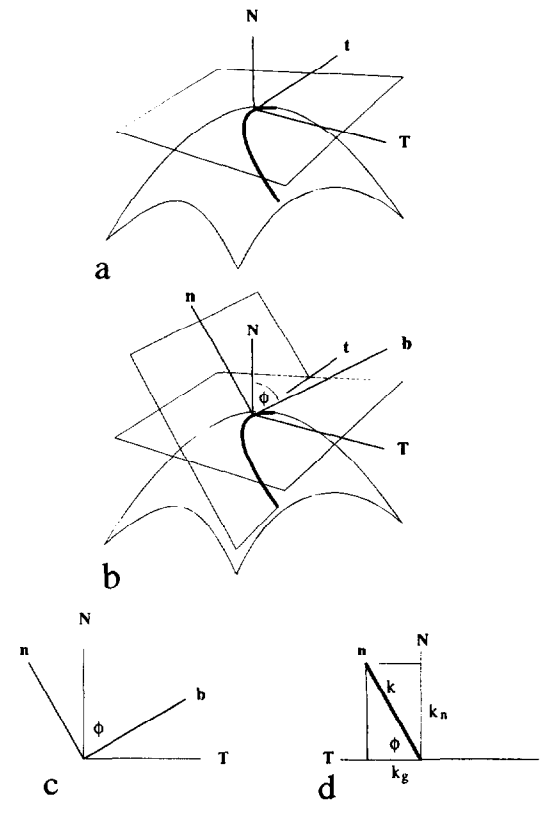

Fig. 4. Surface curves. (a) The surface curve frame defined by the surface normal **N**, the tangent **t** and perpendicular **T**. (b) Surface curve and space curve frames compared. Tangent **t** is shared by both sets. ϕ is the angle between **N** and **b** and describes the relative tilt of both sets of axes. (c) View of frames looking along the direction of **t**. (d) The normal curvature k_n and geodesic curvature k_g are the projections of k onto the **N** and **T** axes, respectively.

The sign of k depends on which side of the curve the centre of curvature lies. The units of k are m^{-1}.

The *torsion of a space curve*, τ at P is a measure of the rate of change in attitude of the osculating plane, with change of s. Alternatively the torsion can be visualized as the rate of change of the binormal vector **b**, as the latter is by definition perpendicular to the osculating plane (Fig. 3b). Torsion is formally defined from:

$$\mathbf{b}' = -\tau\,\mathbf{n} \text{ (Nutbourne \& Martin 1988, p. 24).} \quad (2)$$

A space curve with zero torsion is a *plane curve*.

Surface curves

Ways are now considered of describing the shape of curves which are no longer hanging unsupported in space like those discussed above, but are contained within a flat or curved surface. This is done with the aid of the *surface curve frame* (Fig. 4a) which again consists of three orthogonal axes and a triplet of planes containing pairs of axes (the surface curve trihedron). As with the space curve frame, the curve's tangent defines one axis, **t**. Another axis **N** is the *normal to the surface* and is not to be confused with **n**, the space curve normal. The third orthogonal axis is labelled **T**. The plane containing **t** and **T** is called logically the *tangent plane*; the plane containing **N** and **t** is the *cleaver plane* (Nutbourne & Martin 1988, p. 115).

For any curve that lies on a surface we have two alternative ways of describing its local properties. At any point along it we have the space curve frame and the surface curve frame and their corresponding trihedra.

The two trihedra always share a common axis, the **t** axis, which means that a rotation about this axis can bring the two trihedra into coincidence. The angle ϕ is the rotation required to bring **N**, the surface normal, into coincidence with **b**, the binormal axis of the space curve frame (Figs. 4b & c). If ϕ is 90°, the osculating plane of the curve coincides with the cleaver plane, i.e. **n** is parallel to **N**. If $\phi = 0°$, the curve is an in-plane curve (cf. folded lineations which curve independently of the surface containing them, Ramsay 1967, p. 473).

In general the curvature of the curve, k, can be thought to have two components, the *normal curvature* of the curve (k_n) and the *geodesic curvature* of the curve (k_g), found by resolving k onto two axes of the surface curve frame, **N** and **T** respectively (Fig. 4d). k_n is the curvature of the projection of the curve onto the cleaver plane; k_g is the curvature of the projection of the curve onto the tangent plane. The relative magnitudes of k_n and k_g depend entirely on the angle ϕ, namely

$$k_n = k \sin \phi \quad (3)$$

$$k_g = k \cos \phi. \quad (4)$$

The three measures of curvature are related by:

$$k^2 = k_n^2 + k_g^2. \quad (5)$$

In the space curve frame the torsion τ has been already defined as the rate of rotation of the osculating plane

with distance s along the curve. If the curve lies on a surface the *surface torsion of the surface curve*, τ_g, can also be calculated (Nutbourne & Martin 1988, p. 118):

$$\tau_g = \tau + \phi' \quad (6)$$

where ϕ' is the rate of change of ϕ when moving along the curve, i.e. the relative rotation of the two trihedra per unit distance s along the curve. τ_g is sometimes called the *geodesic torsion of the surface curve*.

Surface curvature and torsion

Defining the curvature of a surface is more complicated than a curve because the former depends on the section plane on which the surface is viewed. To simplify the task we will consider at any point only normal sections of the surface, i.e. the two-dimensional form of the surface as seen on planar sections which contain **N**, the surface normal.

Through any point P on the surface there are an infinite number of curves going off in different directions (Fig. 5a). These curves are all plane curves since they are produced by planar sectioning. They therefore have zero torsion at P and, because their osculating planes are parallel to their respective cleaver planes, their curvatures are equal to the normal curvatures ($\phi = 90°$). It is important to note that if we move away from P, along one of the plane curves, the cleaver plane generally parts company with the osculating plane, thus changing the value of ϕ. At P, the rate of change of ϕ along the curve depends on which plane curve is being considered. With the exception of two special orthogonal curves, ϕ' has a non-zero value. It therefore follows from equation (6) that generally these surface curves have non-zero values of surface torsion ($\tau_g \neq 0$), even though as space curves they possess zero torsion ($\tau = 0$).

Principal curvatures

The normal sections of the surface yield surface curves whose normal curvatures and surface torsions vary in an orderly manner as the direction of the curve through P varies. The extreme values of curvature are associated with two orthogonal directions in the surface called the *principal curvature directions* (Fig. 5b). The values of curvature in these special directions are the *principal curvatures*, k_1 and k_2 where $k_1 \geq k_2$. The principal curvatures may have opposite signs. The principal curvature directions are special in another respect; they possess zero surface torsion.

The Gaussian curvature K, defined as the product of the principal curvatures ($K = k_1 k_2$), is a measure of the amount of double curvature present at a given point in a structure.

Dupin's indicatrix

Dupin's indicatrix is a geometrical representation of the variation of normal curvature of paths through a point P on a surface as a function of the direction of the path, θ. This consists of a curve (Fig. 6) in polar coordinates (R, θ), where $R = 1/k_n^{1/2}$. The radius (R) of the indicatrix in any direction is therefore equal to the square root of the radius of curvature (r) in that direction. Curvature k in any direction is given by: $k_n = 1/R^2$.

The indicatrix is named after Charles Dupin (1784–1873). The equation of Dupin's indicatrix is:

$$k_1 x^2 + k_2 y^2 = \pm 1. \quad (7)$$

The overall shape of the indicatrix depends on the signs of k_1 and k_2:

(a) If the point under consideration is convex or concave with k_1 and k_2 having the same sign, the indicatrix is an ellipse (Fig. 6a).

(b) If the point is saddle-shaped, with k_1 and k_2 having opposite signs, the indicatrix consists of two hyperbolas

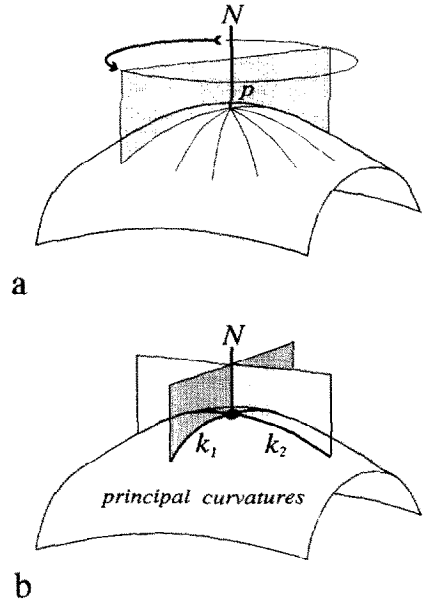

Fig. 5. (a) Normal curvatures of a surface at P vary depending on the direction of the section plane. (b) Principal curvatures k_1, k_2 are the extreme values of curvature at P; they are mutually orthogonal.

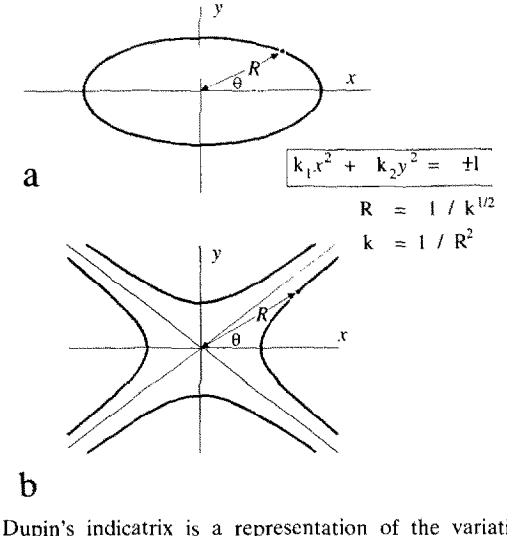

Fig. 6. Dupin's indicatrix is a representation of the variation of normal curvature k with direction of the section plane θ. (a) Elliptical point where k_1 and k_2 have the same sign. (b) Hyperbolic point where k_1 and k_2 have opposite signs.

which have the same asymptotes (Fig. 6b). There are two directions, the *asymptotic directions*, for which the radius of curvature is infinite, i.e. they are straight lines. The latter represents a pair of curves through P, symmetrically arranged with respect to the principal curvature directions, which have zero curvature (Kreyszig 1964, p. 134).

(c) If one of the principal curvatures is zero, the indicatrix consists of a pair of straight lines. The indicatrix indicates that there is now only a single asymptotic direction, one direction with $k = 0$ (i.e. $R = \infty$).

Dupin's indicatrix has another interpretation. If the surface is sectioned by a plane parallel to the tangent plane on a height just above or below P the resulting section has a form which matches closely Dupin's indicatrix. In this way, curvature properties of points on a surface can be deduced from the patterns defined by topographic contours (Koenderink 1990, p. 229) or structure contours (Lisle 1992a). Points on a surface can so be classified as *elliptic, hyperbolic* (or anticlastic) or *parabolic* depending on the conditions (a), (b) or (c) listed above. If the point is hyperbolic, this section exhibits only one of the two hyperbolas constituting the indicatrix. When the indicatrix is a circle, $k_1 = k_2$. Such a point is called an *umbilical point* or *umbilic* (Struik 1961, p. 82). All points on a sphere are umbilical points, on a triaxial ellipsoid there are four umbilical points.

Dupin's indicatrix expresses a surprising property of continuous surfaces: in spite of the infinite variety of forms these can adopt, their local properties are orderly and simple.

Directional variability of normal curvature and surface torsion

A theorem by Leonard Euler published in 1767 expresses the fact that the normal curvature k_n of a chosen line through P can be simply derived from the principal curvatures, (k_1, k_2) and the angle θ, the angle between the considered line and the k_1 principal curvature direction.

$$k_n = k_1 \cos^2 \theta + k_2 \sin^2 \theta. \quad (8)$$

The torsion τ of every curve produced by sectioning the surface at P on planes containing the surface normal N is zero (since each such curve is a plane curve). However for these curves, the *surface* torsion τ_g ($= \tau + \phi'$), which depends on the rotation rates of the space curve and surface curve trihedra, is in general non-zero. The variation of τ_g with θ is expressed by Sophie Germain's formula (see Nutbourne & Martin 1988, p. 170):

$$\tau_g = (k_2 - k_1) \sin \theta \cos \theta. \quad (9)$$

MOHR CONSTRUCTION FOR SURFACE CURVATURE

The section below relies heavily on the description of the "circle diagram for curvature" given by Nutbourne & Martin (1988, pp. 174–180). These authors provide a history of the use of this diagram, to which mention of Jaeger (1966) could be added.

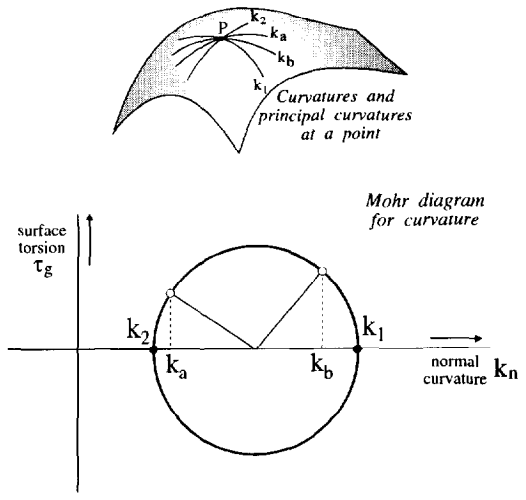

Fig. 7. The Mohr circle for curvature. Each point on the circumference of the Mohr circle represents the normal curvature and surface torsion of a curve through point P on the surface. See text for explanation.

Equations (8) and (9) describe the manner in which the principal curvature values and the direction of a curve (θ) control the values of normal curvature and surface torsion, respectively. They can be re-written in terms of 2θ:

$$k_n = \tfrac{1}{2}(k_1 + k_2) + \tfrac{1}{2}(k_1 - k_2) \cos 2\theta \quad (10)$$

$$\tau_g = -\tfrac{1}{2}(k_2 - k_2) \sin 2\theta. \quad (11)$$

These equations describe the coordinates (k_n, τ_g) of points lying on a circle (Fig. 7), the *Mohr circle for surface curvature and torsion* (Nutbourne 1986). As θ changes, the points defined by the coordinates lie on a circle which is centred on the k_n axis and passes through points k_1 and k_2. The centre of the circle is located at $[\frac{1}{2}(k_1 + k_2), 0]$ and its radius equals $\frac{1}{2}(k_1 - k_2)$.

The Mohr circle serves to illustrate important properties of normal curvatures and surface torsions of surface curves (Fig. 7):

(a) k_1 and k_2 are extreme values of k_n;

(b) principal curvature directions are lines of no surface torsion;

(c) the curves with greatest surface torsion are at 45° to the principal curvature directions;

(d) asymptotic directions (lines with $k_n = 0$), are arranged symmetrically with respect to the principal curvature directions. There will be 2, 1 or 0 asymptotic lines depending on the signs of k_1 and k_2. Figure 8 illustrates the Mohr circles that correspond to elliptical, hyperbolic and parabolic points. The Mohr circle degenerates to a single point in the case of an umbilical point.

The pole of the Mohr circle

By analogy with the Mohr circle for strain (see, for example, Allison 1984, Lisle 1992b), the *pole* of the Mohr circle provides a direct link between the direction

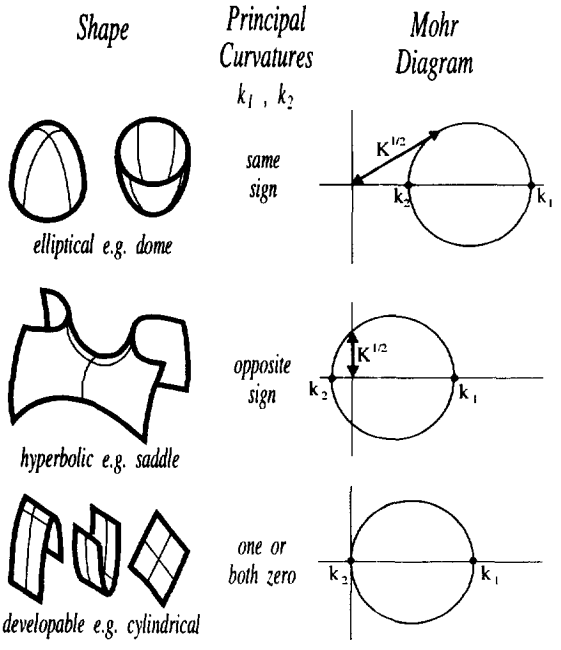

Fig. 8. The signs of the principal curvatures at a point on a surface allow the point to be classified as elliptical, hyperbolic or parabolic (developable). The Mohr circles corresponding to these classes are shown. The value of Gaussian curvature K is given by the square the length of the line labelled $K^{1/2}$ on the Mohr circle. The Mohr circle corresponding to an umbilical point is one with zero radius.

of surface curves in the tangent plane at P and their representation as points on the Mohr circle. To aid understanding of the concept of the pole we consider the Mohr diagram being physically drawn on the tangent plane at P, like a naughty pupil sketching on teacher's mortar board (Fig. 9). The pole is a special point on the circumference of the Mohr circle which has the following property:

> The true orientation of a given curve in the tangent plane is found from its representation as a point on the Mohr circle by joining this point to the pole.

The pole is found as follows (Fig. 9):

> From the right-most point of the Mohr circle (the point labelled k_1) draw a chord across the circle in a direction parallel to that which the k_1 direction has in the tangent plane. The point where the chord cuts the circumference is the pole of the Mohr circle.

Once the position of the pole is established, the k_n and τ_g values of any curve through P are readily found:

> Through the pole draw a chord of the Mohr circle in the real orientation of the curve under consideration. The chord meets the circle at the point k_n, τ_g.

It should be noted that the use of the pole in this way implies a sign convention for τ_g which is the opposite of that used by Nutbourne & Martin (1988, p. 171).

Finding the principal curvatures

The Mohr circle construction can be applied to determine the directions and magnitudes of the principal curvatures from values of normal curvature measured in a number of random directions through a point on a surface. Since the problem is analogous to the solution of the strain ellipse from strain rosette data, a similar method can be used. Such a method is described by Lisle & Ragan (1988).

PRINCIPAL CURVATURE TRAJECTORIES

Any path on a surface always tangent to a principal curvature direction is called a *line of curvature* or *principal curvature trajectory*. On any curved surface we can imagine two mutually orthogonal sets of such trajectories: one tracking k_1, the other following k_2.

The surface torsion is, by definition, zero everywhere along a principal curvature trajectory. This means that

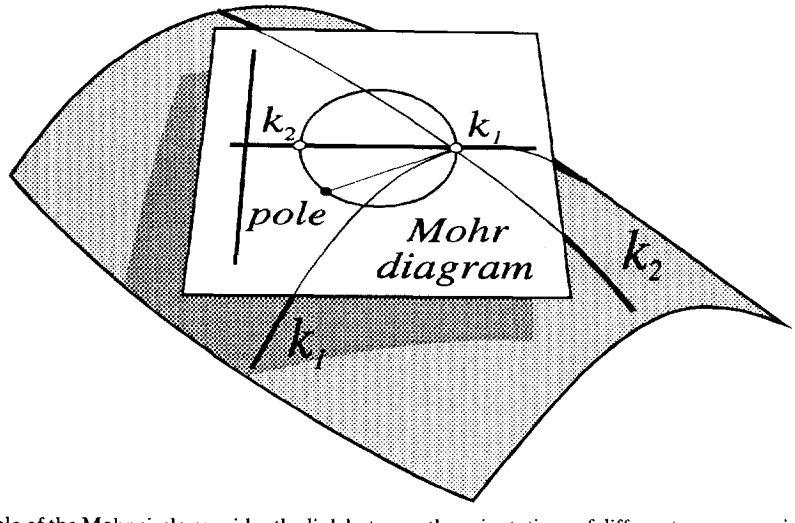

Fig. 9. The pole of the Mohr circle provides the link between the orientations of different curves passing through a point on a surface and the representations of those lines as points on the Mohr diagram. Imagine the Mohr diagram is drawn on the tangent plane to the surface at a point on the surface. The pole of the Mohr circle is found by drawing a chord across the circle in a direction parallel to a principal curvature direction (e.g. k_1) and through the point on the Mohr circle representing that principal direction (point labelled k_1). Once located, the curvature properties of any surface curve (portrayed as a point on the circle's circumference) are found by drawing a chord through the pole in the direction of the considered curve.

the surface normal vector **N** may tip forwards or backwards as the curve progresses, but it may not tilt sideways (Nutbourne & Martin 1988, p. 125).

The directions of trajectories are not defined at flat points on a surface. The same is true at umbilical points.

PRACTICAL CURVATURE ANALYSIS

A method is here described for calculating principal curvature trajectories for any folded surface. The method requires knowledge of the elevation of the folded surface at points arranged on a square grid. Curvatures are calculated at each non-peripheral node of the grid using the height of the grid point in relation to the eight nearest neighbours (Fig. 10):

(a) These points are considered three at a time; the central grid node and a pair of opposing neighbours. The three points together define a space curve with a vertical osculating plane and a horizontal **b** vector. Curvature k of this curve is calculated by finding the radius of a circular arc passing through three points in a plane (see Appendix).

(b) Four such curvatures, k_a, k_b, k_c and k_d referring to four different vertical sections can be calculated through the grid node. The orientations of the **b** vectors of successive curves differ by 45° from each other.

(c) To be able to convert these curvatures into normal curvatures the local orientation of surface normal first has to be determined. The average attitude of the surface at the node, and hence its normal vector **N**, is found by least-squares fitting of the node together with its eight neighbours to a plane (see, for example, Ferguson 1988, pp. 102–104).

(d) For each plane curve the angle ϕ can be found, being the angle between **N** and **b**. This permits the curvatures k_a, k_b, etc. to be converted into normal curvatures k_{na}, k_{nb}, etc. by applying equation (3).

(e) From the information available at each node, i.e. four normal curvatures k_{na}, k_{nb}, etc. and their corresponding directions θ_a, θ_b, etc., the Mohr circle for curvature is constructed using the procedure set out in Lisle & Ragan (1988). This involves finding the best-fit circle through four points on the Mohr diagram using a least-squares method (Lisle 1992c).

(f) Once the Mohr circle has been constructed, the principal curvatures k_1 and k_2 are fixed, and their directions are simply determined using the pole.

(g) Steps (a)–(f) are repeated for each grid node.

Quite clearly, the above calculations necessitate the application of a purposely written computer program. A version of the program being developed by one of us (JR) will allow the computation of principal curvatures from sets of data points (x,y,z) which are spaced irregularly across the surface.

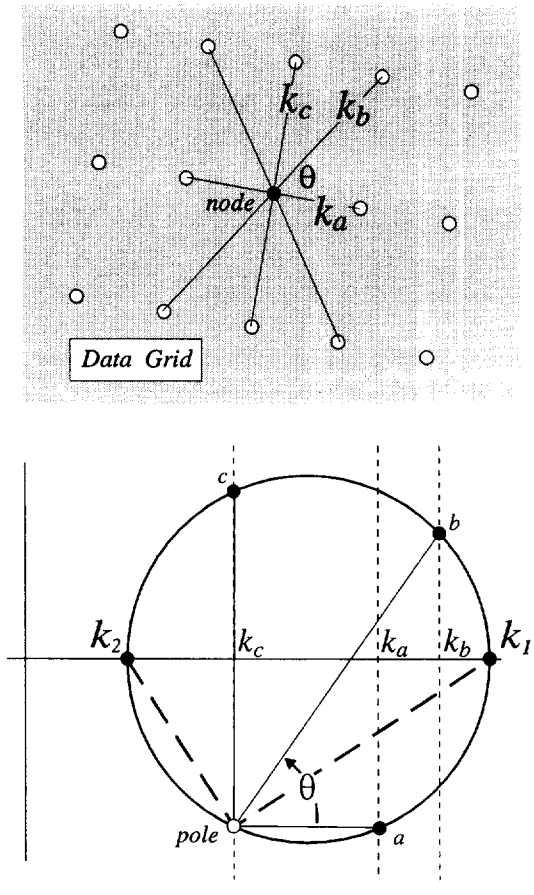

Fig. 10. Method used to calculate curvatures on a surface for which known elevations are arranged on a regular grid. Curvatures are calculated in specific grid directions using the heights of three points; the node plus a pair of opposing neighbours. Principal curvatures are found by Mohr construction using the 'strain-rosette method' of Lisle & Ragan (1988). See text for explanation.

EXAMPLES OF CURVATURE ANALYSIS

Goose Egg Dome, Wyoming

To illustrate the proposed method an example is taken of the non-cylindrical Goose Egg Dome in the foothills of the Rockies in Wyoming. The structure consists of a periclinal anticline with approximate dimensions 4 and 2 km, which folds a sequence of Mississippian–Cretaceous sediments. The structure is described by Harris *et al.* (1960) from which the structure contour map of the top Pennsylvanian (Fig. 11) is taken. The structure contour pattern confirms the non-cylindrical geometry of the anticline and of an adjoining saddle structure to the east. The overall elliptical shape of the contours suggests that the periclinal anticline has a direction of absolute least curvature in a roughly east–west direction and positive Gaussian curvature (Lisle 1992a). This type of deduction warrants caution however since the type of contour shape (elliptical, hyperbolic, etc.) is a reliable indicator of the curvature present only at small portions of the structure, namely, in the vicinity of the points where the tangent plane to the structure is horizontal; at crest points, saddle points and trough points on the structure (Lisle in press).

A more meaningful description of the structure comes from a survey of principal curvatures across the structure. A square grid was superimposed on the structure

contour map in Fig. 11 and the elevations at the grid nodes interpolated. The estimation of heights of the surface in this manner is a significant source of error as the original data on which the stratum contours were based and our estimations of elevations are separated by two stages of interpolation. The calculation of curvatures, a quantity related to the second derivative of the surface, will be sensitive to such errors. This must detract from the quality of our analysis of curvature in this example. The calculation of the principal curvatures and their directions at each grid node was carried out using the computer program (which incorporates the Mohr construction) described above. The results of the curvature analysis of the Goose Egg structure are displayed on two maps; the Gaussian curvature map (Fig. 11) and the curvature trajectory map (Fig. 12).

Gaussian curvature (K) is the measure of the degree and type of double curvature present. It is calculated as the product of the principal curvature values derived from the Mohr circle method, i.e. $K = k_1 k_2$. A cylindrical fold, for example, would consist entirely of parabolic points (points with $K = 0$) since at every point one of the principal curvatures is zero. The value of K is however not on its own an appropriate indicator of the deviation from cylindrical fold geometry since cylindrical folds are just one member of a class of fold surfaces called developable surfaces which consist entirely of points with $K = 0$ (Lisle 1992a). An additional property of cylindrical folds is the parallelism of the minimum absolute principal curvature axes. Figure 11 shows the calculated values of Gaussian curvature across the region and highlights those areas where the structure deviates most from developable geometry. These are the vicinity of the crest of the dome where K is positive (dark grey shading), the saddle structure to the east (especially the north side) where K is negative (light grey shading) and minor patches on the S flank of the dome where the transverse synclinal furrows are superimposed on the overall convex upwards shape. The Gaussian curvatures calculated accord closely with those found by the angular defect method, an independent technique for estimating K (Lisle in press).

Gaussian curvature is a geometrical descriptor of fold shape which expresses the surface's departure from a *developable* geometry. Developable surfaces, which include cylindrical-, conical- as well as some other ruled-surfaces, are geometries that can develop from folding of a non-stretching sheet, termed isometric folding by Lisle (1992a). The Gaussian curvature is zero at every point on such surfaces. The importance of Gaussian curvature measurement therefore lies in its potential to indicate portions of a structure with non-developable shapes which, for their formation, must have involved bed-stretching. The use of Gaussian curvature analysis as a tool for predicting strains (fracture densities) in the Goose Egg structure is the subject of a separate paper (Lisle in press).

The curvature trajectory map (Fig. 12) shows the calculated principal directions of curvature across the structure. The directions shown are the axes of least curvature in absolute terms (regardless of sign). For cylindrical folding these directions would be parallel to the fold axes, so each direction can be visualized as the 'best local fold axis'. The term fold axis is used here loosely because the term is only formally defined for ideal cylindrical folds. The trajectory map reveals a more variable pattern of folding that would be appreciated from inspection of the structure map. The crestal region of the dome for example is clearly a patch of more variable curvature directions than the apparently simple oval pattern of the structure contours would suggest. The method highlights the significance of modest embayments of the contours on the S flank of the dome. The local curvature axis can be transverse to the macroscopic trend of the structure, e.g. in the area of the saddle. Besides these, there are other portions of the map where the calculated curvature directions are locally variable. There are two likely explanations for this; firstly the imprecise data on the elevations of the surface, and secondly the existence of patches on the structure with approximately umbilical curvature, i.e. $k_1 = k_2$.

The curvature trajectory map (Fig. 12) provides the equivalent of the 'tectonic cross', a reference set of axes used to describe orientation in relation to cylindrical structures. For non-cylindrical folds a set of three orthogonal axes, comprising the local principal curvature axes, k_1, k_2, and the surface normal **N**, provides a more meaningful local reference frame for observations on small-scale structures such as fracture patterns, cleavage orientations and palaeostress axes. In the case of the Goose Egg structure, this local reference frame is clearly variable in direction. Any minor structures maintaining a fixed orientation with respect to this local frame would show a highly variable relation with any global external tectonic cross for the structure.

Fold from Laksefjord, N. Norway

A second example is taken of a hand specimen of a band of quartzitic gneiss collected from northern Norway. The fold (Fig. 13a) is clearly non-cylindrical at one end, where its amplitude decreases. The dimensions of the fold are approximately 25 cm by 14 cm.

A grid of elevations of the surface of the fold was obtained by sliding the fold around on a fixed sheet of graph paper beneath a fixed rig from which the elevations could be measured. The grid spacing was 8 mm; the elevations were read to 0.1 mm with an estimated error of ± 0.2 mm. The calculation of the Gaussian curvatures and the principal curvatures and their directions was carried out directly on these measurements using the Mohr construction method. This avoids the problems of using interpolated data. The results of the curvature analysis of the Norway fold are displayed on two maps, one showing the structure contours and curvature trajectories (Fig. 13b) and the other showing Gaussian curvatures (Fig. 13c). Both maps display the curvature trajectories.

Figure 13(c) shows that the highest values of Gaussian curvature occur in the northwest part of the map, this

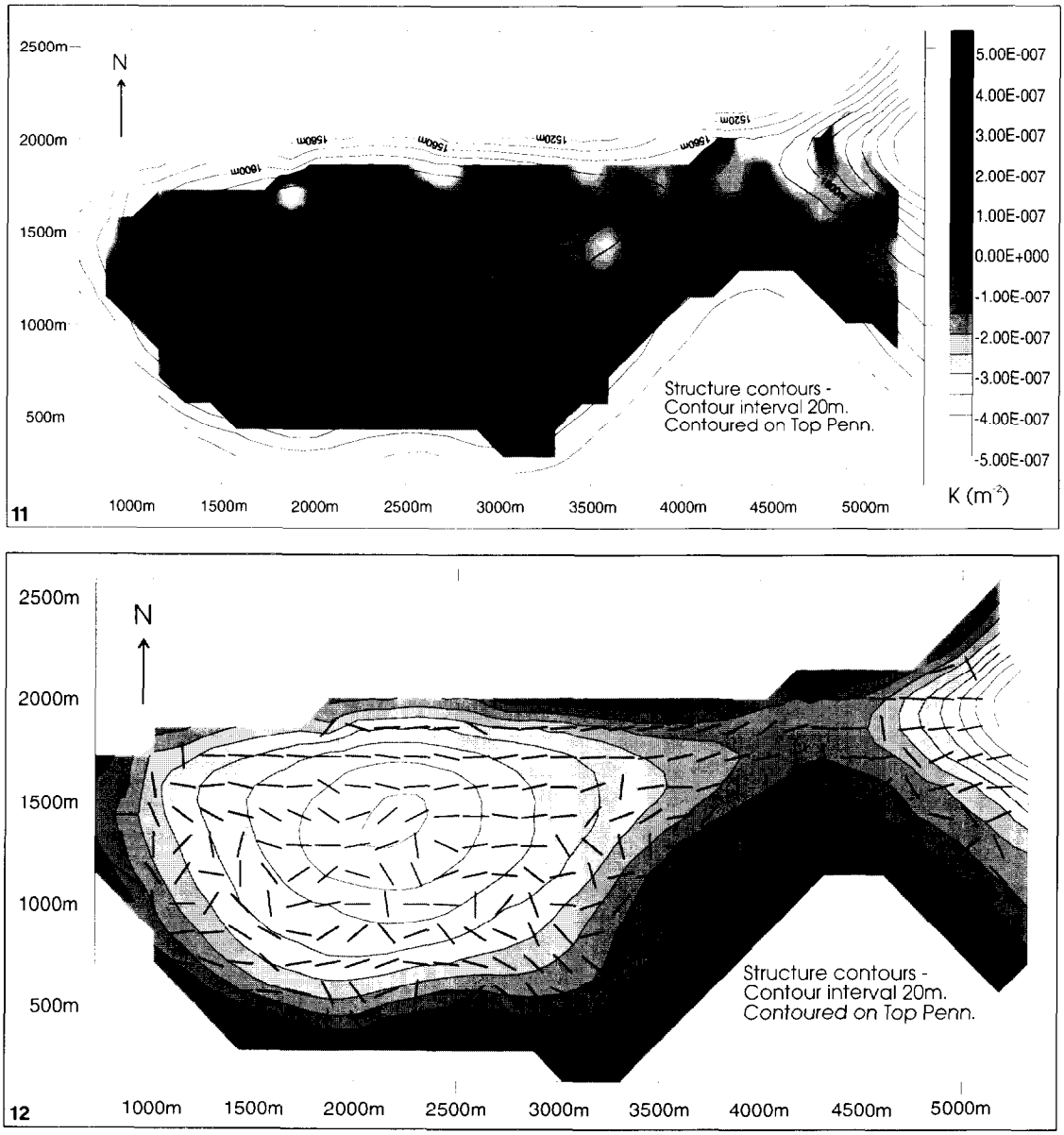

Fig. 11. The Goose Egg Dome, Natrona County, Wyoming. The black lines are the structure contours for the top Pennsylvanian taken from Harris *et al.* (1960). Grey shades indicate the absolute values of Gaussian curvature ($K = k_1 k_2$) calculated using the Mohr circle method.

Fig. 12. Curvature trajectory map for the top Pennsylvanian in the Goose Egg Dome. The dashes are the directions of the principal curvature axis with the least absolute magnitude. These directions can be thought of as the 'best local fold axes'.

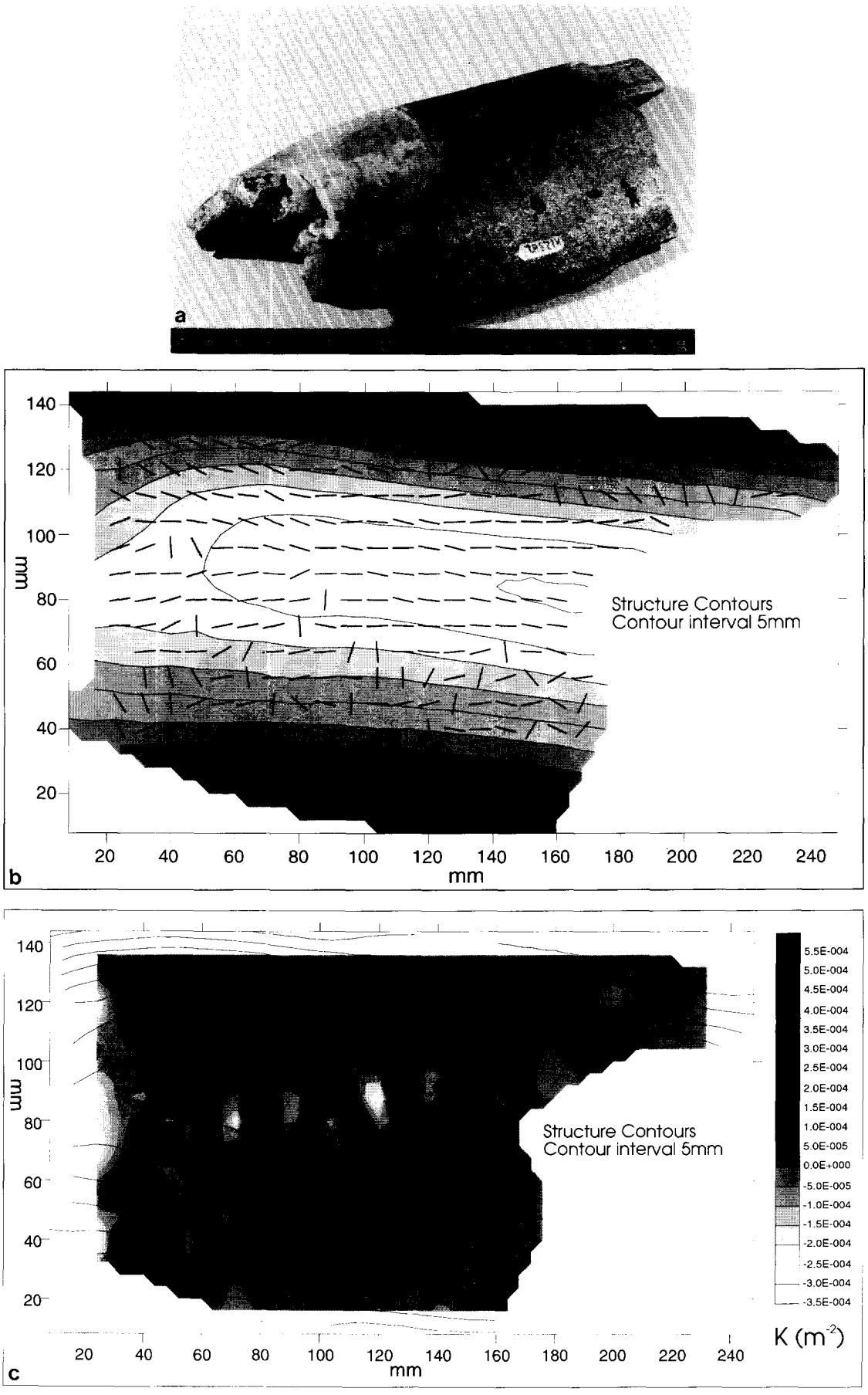

Fig. 13. Laksefjord Fold (a) the folded surface. (b) Structure contour map and curvature trajectories (principal directions of minimum curvature). (c) Gaussian curvature map with superimposed structure contours.

corresponds with a visible doming of the surface, i.e. the surface is notably curved in all directions (compare Fig. 13a). The lowest (negative) values of Gaussian curvature occur where there are shallow saddle points along the major fold axis where the maximum principal curvature direction is perpendicular to the major fold axis and where the minimum principal curvature axis corresponds to gentle undulations of the major fold axis. The low values of K at the far west end of the major fold axis is where an obvious saddle occurs. It is to be noted that filled fractures with transverse orientation (visible in Fig. 13a) occur in a region of high Gaussian curvature represented by the darkest shading at $x = 80$ mm, $y = 85$ mm on Fig. 13(c).

The curvature trajectories for the Norway example, the axes of least curvature, show a large variation across the structure (Figs. 13b & c). The curvature trajectories parallel the major fold axis along the crest of the fold, as would be expected; however the trajectories on the limbs, especially the southern limb, are more variable in trend. This is because the limbs are largely uniformly dipping with very small curvatures. Many of the trajectories on the north limb lie perpendicular to the major fold crest line, highlighting modest embayments of the structure contours on this limb. In the northwest of the structure, in the region of the high positive Gaussian curvature values it is interesting to note how the curvature trajectories progressively swing around from EW-trending to NW-trending.

CONCLUSIONS

(1) The description of the form of non-cylindrically folded surfaces requires the specification of more parameters than in the case of cylindrical folds. Familiar concepts such as fold hinge, fold axis lose their validity when applied to non-cylindrical structures.

(2) Non-cylindrical folds can be described by means of maps showing the variation of local curvature attributes of the surface: the principal curvature directions and their magnitudes.

(3) The analysis of local curvature properties and the calculation of principal curvatures on folded surfaces are readily performed by means of the Mohr construction for curvature.

(4) Principal curvature trajectory maps provide at all points across a surface a local fold reference frame. These reference directions could assist in the analysis of structures produced by interfering fold sets and of fracture patterns in non-cylindrical structures.

(5) A correlation is observed in the Norwegian example between the location of discontinuities (fractures) in the surface and the occurrence of strongly non-zero Gaussian curvature values.

Acknowledgements—This work was carried out as part of an extramural research contract with Shell Research, Rijswijk, Holland. The work profited from discussions with Mike Naylor and Ramon Loosveld (both of Shell) and Ralph Martin (Department of Computing Mathematics, University of Wales, Cardiff). Useful suggestions on the manuscript were made by Robert J. Twiss and an anonymous referee. Steven Wojtal drew our attention to the work of Jaeger (1966).

REFERENCES

Allison, I. 1984. The pole of the Mohr diagram. *J. Struct. Geol.* **6**, 331–333.

Calladine, C. R. 1986. Gaussian curvature and shell structures. In: *The Mathematics of Surfaces* (edited by Gregory, J. A.). Clarendon Press, Oxford, 178–196.

Ferguson, J. 1988. *Mathematics in Geology*. Allen and Unwin, London.

Harris, J. F., Taylor, G. L. & Walper, J. L. 1960. Relation of deformational structures in sedimentary rocks to regional and local structure. *Bull. Am. Ass. Petrol. Geol.* **44**, 1853–1873.

Hilbert, D. & Cohn-Vossen, S. 1932. *Geometry and the Imagination*. Chelsea Publishing Company, New York (reprinted 1983).

Jaeger, L. G. 1966. *Cartesian Tensors in Engineering Science*. Pergamon, Oxford.

Koenderink, J. J. 1990. *Solid Shape*. MIT Press, Cambridge, Massachusetts.

Kreyszig, E. 1964. *Differential Geometry*. University of Toronto Press, Canada.

Lipschutz, M. M. 1969. *Theory of Problems of Differential Geometry*, Schaum's Outline Series. McGraw-Hill, New York.

Lisle, R. J. 1992a. Constant bed-length folding: three-dimensional geometrical implications. *J. Struct. Geol.* **14**, 245–252.

Lisle, R. J. 1992b. Strain analysis by simplified Mohr circle construction. *Annals Tectonicae* **5**, 102–117.

Lisle, R. J. 1992c. Least squares best-fit circles (with applications to Mohr's diagram). *Mathematical Geology* **24**, 455–461.

Lisle, R. J. In press. Detection of strain in structures using Gaussian curvature analysis. *Bull. Am. Ass. Petrol. Geol.*

Lisle, R. J. & Ragan, D. M. 1988. Strain from three stretches—a simple Mohr Circle solution. *J. Struct. Geol.* **8**, 905–906.

Nutbourne, A. W. 1986. A circle diagram for differential geometry. In: *The Mathematics of Surfaces* (edited by Gregory, J. A.). Clarendon Press, Oxford, 59–72.

Nutbourne, A. W. & Martin, R. R. 1988. *Differential Geometry Applied to Curve and Surface Design*, Vol. 1, Foundations, Ellis Horwood, Chichester.

O'Neill, B. 1966. *Elementary Differential Geometry*. Academic Press, New York.

Ramsay, J. G. 1967. *Folding and Fracturing of Rocks*. McGraw-Hill, New York.

Struik, D. J. 1961. *Lectures on Classical Differential Geometry*. Addison-Wesley, Reading, Massachusetts.

Suppe, J. 1985. *Principles of Structural Geology*. Prentice-Hall, Englewood Cliffs, New Jersey.

Turner, F. J. & Weiss, L. E. 1963. *Structural Analysis of Metamorphic Tectonites*. McGraw-Hill, New York.

APPENDIX: THE CIRCLE PASSING THROUGH THREE CO-PLANAR POINTS

Choosing one of the three points as the origin, the problem involves finding the circle with centre (x_c, y_c) passing through points (0,0), (x_1, y_1) and (x_3, y_3). Referring to Fig. A1, chord 1 has slope y_1/x_1 and its perpendicular therefore has a slope, $m = -x_1/y_1$.

In the equation of the perpendicular bisector of chord 1 ($y = mx + c$) the constant c can be evaluated because this perpendicular passes through the point $(\frac{1}{2}x_1, \frac{1}{2}y_1)$:

$$\tfrac{1}{2}y_1 = (-x_1/y_1)\tfrac{1}{2}x_1 + c.$$

Therefore, $c = \frac{1}{2}(y_1 + x_1^2/y_1)$.

The equation of the perpendicular 1 is therefore:

$$Y = (-x_1/y_1)X + \tfrac{1}{2}(y_1 + x_1^2/y_1). \quad \text{(A1)}$$

The equation of the perpendicular bisector of chord 2 can be found in a similar fashion to be:

$$Y = (-x_3/y_3)X + \tfrac{1}{2}(y_3 + x_3^2/y_3). \quad \text{(A2)}$$

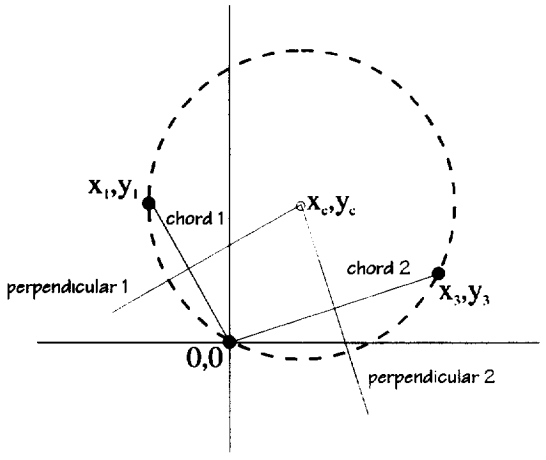

Fig. A1. Finding the centre x_c, y_c of the circle passing through three co-planar points x_1, y_1 $x_2 = 0$, $y_2 = 0$ and x_3, y_3.

The centre of the circle (X_c, Y_c) is found at the intersection of the perpendiculars to chords 1 and 2 and its coordinates by the solution of simultaneous equations (A1) and (A2).

This gives:

$$Y_c = (t_1 t_2 + t_3)/(1 + t_1) \tag{A3}$$

where $t_1 = -(x_1 y_3)/(y_1 x_3)$, $t_2 = \frac{1}{2}(y_3 + x_3^2/y_3)$, $t_3 = \frac{1}{2}(y_1 + x_1^2/y_1)$ and

$$X_c = (y_3/x_3)(-Y_c + t_2). \tag{A4}$$

Special cases

(a) When $y_1 = 0$, X_c equals $\frac{1}{2}x_1$ which is substituted for in equation (A2) to give Y_c.

(b) When $y_3 = 0$, X_c equals $\frac{1}{2}x_3$ which is substituted for in equation (A2) to give Y_c.